NASA CONTRACT NAG8-098

FINAL PROGRESS REPORT
March 31, 1989

NOVEL PROTEIN CRYSTAL GROWTH TECHNOLOGY

PROOF OF CONCEPT

THOMAS A. NYCE AND FRANZ ROSENBERGER

CENTER FOR MICROGRAVITY AND MATERIALS RESEARCH

University of Alabama in Huntsville

Huntsville, Alabama 35899

ABSTRACT

This is the year end report on research done under NASA Grant NAG8-098 and covers the period from Dec 1, 1987 to March 31, 1989. Originally proposed for one year, the research conducted between Jan 1, 1989 and March 31, 1989 was under a no-cost extension of this grant.

The purpose of this project was to develop a new technology for crystal growth, which overcomes certain shortcomings of other techniques, and to examine in particular its applicability to proteins. The basic idea is to suspend a growing crystal in a specially configured upflow of supersaturated nutrient, which is provided by the effect of fluid bouyancy in a closed loop thermosyphon. There were several unknowns to be determined: the design of the apparatus for suspension of crystals of varying (growing) diameter, control of the temperature and supersaturation, the methods for seeding and/or controlling nucleation. Furthermore, the effect on protein solutions of the temperature oscillations arising from the circulation and the effect of the fluid shear on the suspended crystals was unknown.

As reported in the first semi-annual report: an estimate of the velocities necessary to suspend the crystals was made; the angle of expansion and size of the growth chamber was determined; two crystal growth apparatuses were designed and built; and a "growth protocol" was developed using readily available inorganic materials. Since then, extensive effort was put forth to grow lysozyme crystals using this technology. Under conditions favorable to the growth of tetragonal lysozyme, spontaneous nucleation could be produced but the number of nuclei could not be controlled (a common and serious problem in protein crystal growth). Hence, seed transfer techniques were developed and implemented. Although the suspension of the seeds worked very well, there was no measurable growth. On the other hand, seeds from the same source, when transferred into a stagnant control solution, grew readily. When conditions for the orthorhombic form were tried, a single crystal 1.5mm x 0.5mm x 0.2 mm was grown (after in situ nucleation) and successfully extracted. Several lysozyme crystals of a size appropriate for x-ray crystallography were grown under these conditions.

A mathematical model was developed to predict the flow velocity as a function of the geometry and the operating temperatures. Good agreement with flow rates measured in the apparatus was observed. This model shows

a lower limit on the amount of solution required for this method. The model can also be used to scaleup the apparatus for growing larger crystals of other materials such as water soluble non-linear optical materials.

The initial stages of the patenting process for this new technology are underway. Whether other proteins would grow successfully in the apparatus can only be determined by further experiments. This crystal suspension technology also shows promise for high quality solution growth of optical materials such as TGS and KDP.

Table of Contents

1. Introduction

The goal of this research was to develop a new technology for crystal growth in which crystals are freely suspended in the nutrient solution, eliminating container wall contact and maximizing the uniformity in solute supply to the interface. In particular, the applicability of this technology to the growth of protein crystals was to be explored. The basic idea is to suspend a growing crystal in a specially configured upflow of supersaturated nutrient, where the upflow is provided by the effect of fluid buoyancy in a closed loop thermosyphon. Several unknowns were to be determined: the design of the apparatus for suspension of crystals of varying (growing) diameter, control of the temperature and supersaturation, the methods for seeding and/or controlling nucleation. Additionally, the effect of the temperature oscillations arising from the circulation of the (protein) solutions and the effect of the fluid shear on the suspended crystals were unknown.

For the purpose of this report the research has been divided into two major categories: design and crystallization. Section 2 deals with the prediction of velocities required to suspend the crystals, and the design of the apparatuses. Section 3 describes the crystallization schemes and results of the experimental runs. A summary is presented in Section 4.

2. Design Results and Guidelines

2.1 Particle Suspension Dynamics

The primary quantity to be determined here is the flow velocity required to suspend the crystals as they grow. When this upward velocity is equal to the rate at which the crystal would settle in a motionless fluid, the crystal will be suspended. Additionally, several types of instabilities in the position and orientation of the crystal are possible because the crystals are nonspherical and they grow into a size range above that for Stokes flow. These instabilities must be avoided to reduce the chance of particles hitting the walls of the chamber. The main design problems are that the evaluation of settling rates for nonspherical particles is not well established and that individual crystals may have a variety of different shapes. Hence, the calculations for suspension velocities can give only general guidelines and actual experimental trials must be relied on heavily.

If we consider a solution supersaturated enough to produce spontaneous nucleation, the supercritical nuclei are small enough to be in the Stokes law region (particle Reynolds number $Re_p < 0.03$) [1]. As they get larger and their settling velocity increases, they will enter the "intermediate law" region [2]. Figure 1 shows terminal settling velocities for spheres up to 1mm using the physical properties of a typical protein growth system:

particle density $\rho_p = 1.2$ gm/cm^3,

solution density $\rho = 1.02$ gm/cm^3 (density of 3% NaCl solution at 20 °C),

viscosity $\mu = 0.0105$ gm/s•cm.

This figure shows that a protein crystal grown to a size range large enough for x-ray diffraction (0.3 to 1 mm) will be settling in the intermediate law region. Although these corresponding relations were developed for spherical particles, Figure 1 can give useful estimates of the necessary velocities for the operating parameter of the thermosyphon apparatus such that seeds can be trapped or crystals of different sizes can be "weeded out". This will be discussed in more detail later. For predicting these velocities in systems with physical properties other than those shown above, see [1] for the Stokes law region and [2] for the intermediate law region.

As the size of a crystal increases, its settling velocity depends more on its specific shape and the relations for spherical particles used above become increasingly inaccurate. Also, the drag (and thus the velocity) of a nonspherical particle depends on its orientation with respect to the direction of motion. The orientation in free fall as a function of the particle Reynolds number (based on diameter of a sphere of equal surface area) is given in the following table [3].

Reynolds number	Orientation of the Particle
0.1 - 5.5	All orientations are stable when the particle has three or more perpendicular axes of symmetry
5.5 - 200	Stable in the position of maximum drag
200 - 500	Unpredictable. Disks and plates tend to wobble, while fuller bluff bodies tend to rotate
500 - 200,000	Rotation about axis of least inertia, frequently coupled with spiral translation

Table 1. Free Fall Orientation of Particles.

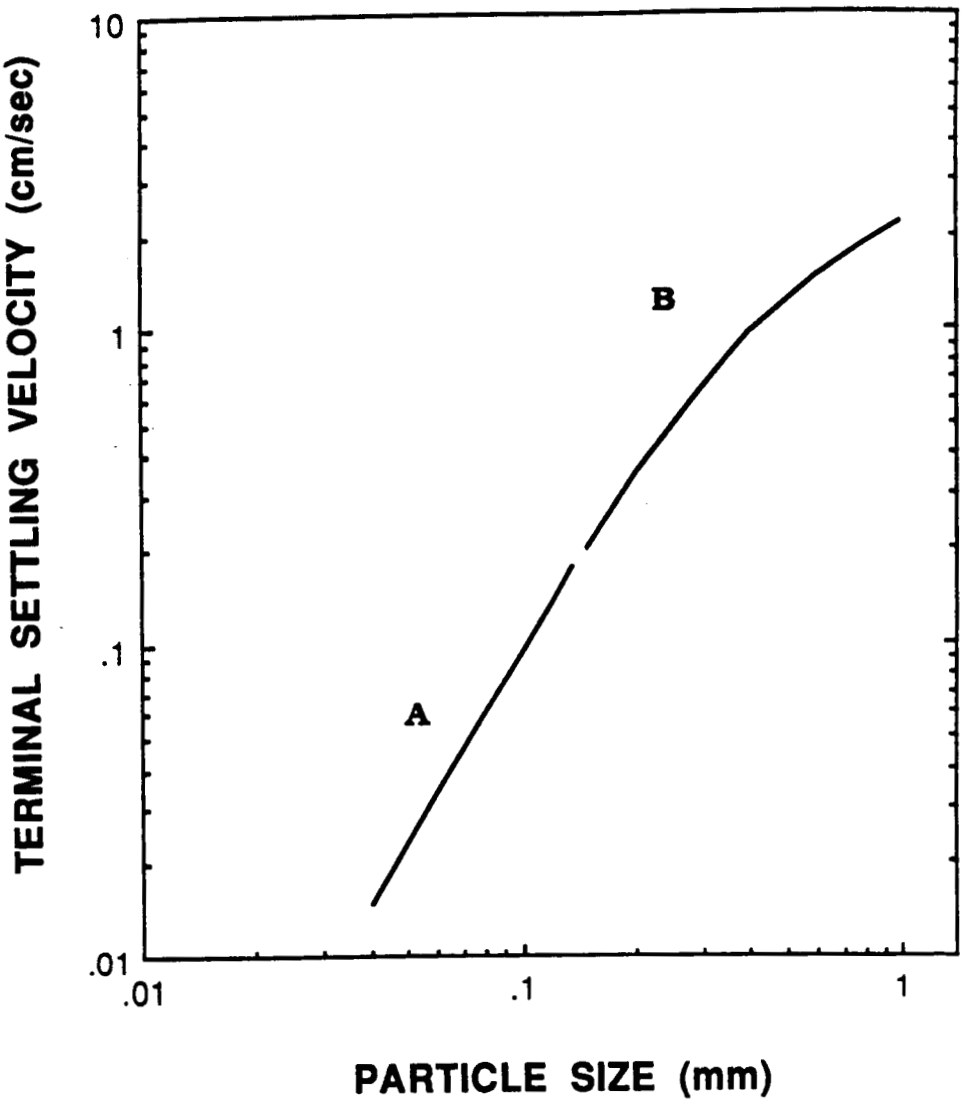

Figure 1. Terminal settling velocities of spheres in A) the Stokes region and B) the intermediate region.

Since the shapes of crystals of a material can vary widely, depending on the growth conditions, experiments must be relied on for the determination of the "falling" orientation and the required suspension velocity.

It must be noted that the above correlations are for bodies settling in a free fluid with no walls. If, however, a particle is settling in a tube the presence of a wall increases drag on the particle [4] and thus reduces the upward velocity required to suspend it. If the particle diameter is 10% of the tube diameter, its settling velocity is 20% less than in an infinite fluid and the pressure distribution in the annular space will tend to center the particle. This wall effect can be used to advantage by making the diameter of the suspension chamber less than ten times the final desired size of the crystal.

2.2 Design of the Expansion Chamber

The design of the expansion chamber itself is critical. The velocity in the smallest part of the chamber must be large enough to suspend the largest size of crystal desired and the velocity in the largest part must be small enough to trap nuclei or seed crystals of a very small size. To minimize the chance of the crystals hitting the wall, the flow in the chamber must be steady, axisymmetrical, and without recirculation in the vicinity of the crystal. We have performed experiments to determine flow rates, tube diameters, and angles of expansion that would be necessary to suspend the crystals. As the expansion chambers and particles used in these experiments were described in the semi-annual progress report, only the primary results are given here.

The onset of recirculation corresponds directly to a "bouncing" motion of the particle resulting in repeated contact with the chamber wall. In all the chambers made from volumetric pipets, recirculation occurred in the flow rate range of 6-8ml/min. These rates depend on the angle of expansion, larger angles showing recirculation at lower velocities, and were independent of the entering tube diameter. This is important because a chamber with a smaller entering tube has a much higher velocity for the same flow rate and, thus, will support a larger particle. The chamber, designed using the information from these experimental studies, is shown in Figure 2. With this chamber, particles in the size range of most interest in protein crystallization (0.4-1mm) were suspended in the velocity range of

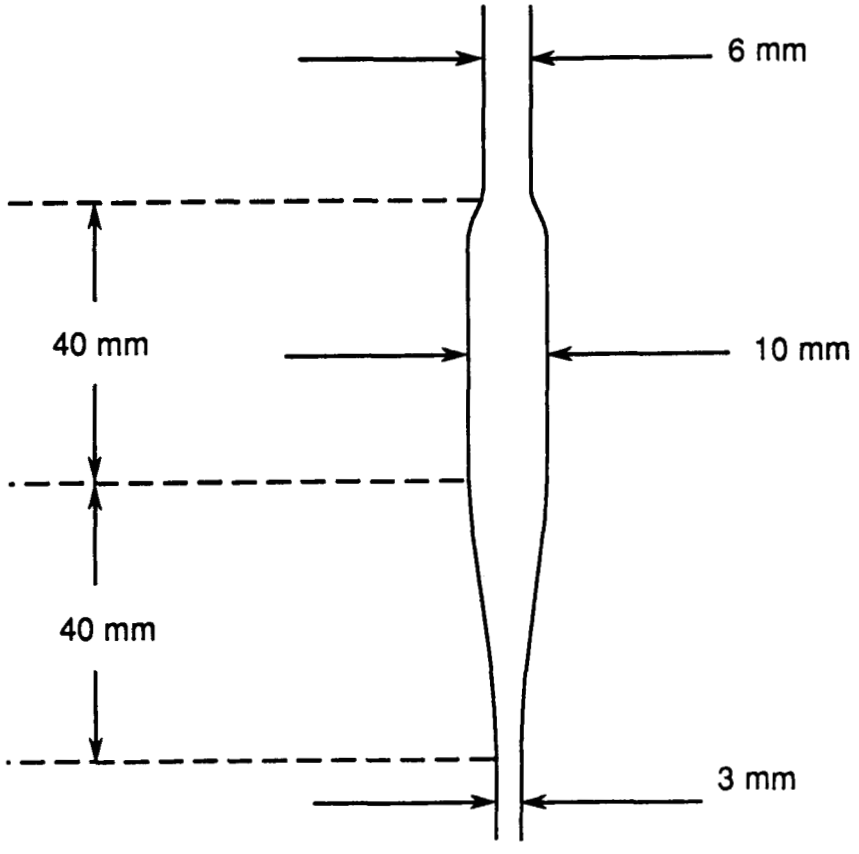

Figure 2. The expansion and growth chamber. Section lengths and inner diameters.

0.5-1.5 cm/s (based on the 3mm part of the chamber). This velocity was then used as part of the design criteria for the thermosyphon loop.

2.3 Circulation Rates and the Design of the Thermosyphon Loop

The design of the thermosyphon loop entails many factors. The flow rate is of primary concern. As discussed above, the narrowest part of the expansion chamber requires a flow velocity large enough to suspend a crystal of the final desired size. The temperature distribution in the loop must be such that nowhere the working limit of the solution is exceeded (many proteins denature at 50°C or below), the appropriate temperature for growth in the expansion chamber is provided, and nucleation elsewhere in the loop is reduced. The design must also minimize the total volume of solution and, thus, the amount of protein used. In general, larger diameter tubes decrease friction in the loop and increase the flow velocities at a given ΔT, but this increases the amount of fluid required in the apparatus. Another important consideration is to avoid the instabilities associated with thermosyphon loops [5-10] which are generally more prevalent when using large diameter tubes at high heating rates.

The majority of theoretical and experimental analyses that deal with thermosyphons use very simplified geometries. There is a great deal of theoretical and experimental work on the "closed loop toroidal thermosyphon" [7-10] which, although not directly applicable to our more complex geometry, can provide useful insight and guidance. As described in more detail in the semi-annual progress report, relations from Creveling et al. [7] were used to provide an estimate of the tube diameter required for the desired flow velocity. A thermosyphon loop was constructed using 10mm inner diameter tubing and incorporating one of the test expansion chambers mentioned above. The velocities in this loop were significantly higher than those predicted by the relation of [7]. In light of these results, it was decided that the first crystal growth thermosyphon apparatus would be made of 6mm ID tubing for the majority of its length.

The crystal growth apparatus, shown in Figure 3, was constructed using the design information given in previous sections of this report. A concentric cooling jacket surrounds the right side of the loop, while the left side is heated by windings of copper constantan wire connected to a controlled current supply. Both the heated and cooled sections of the loops

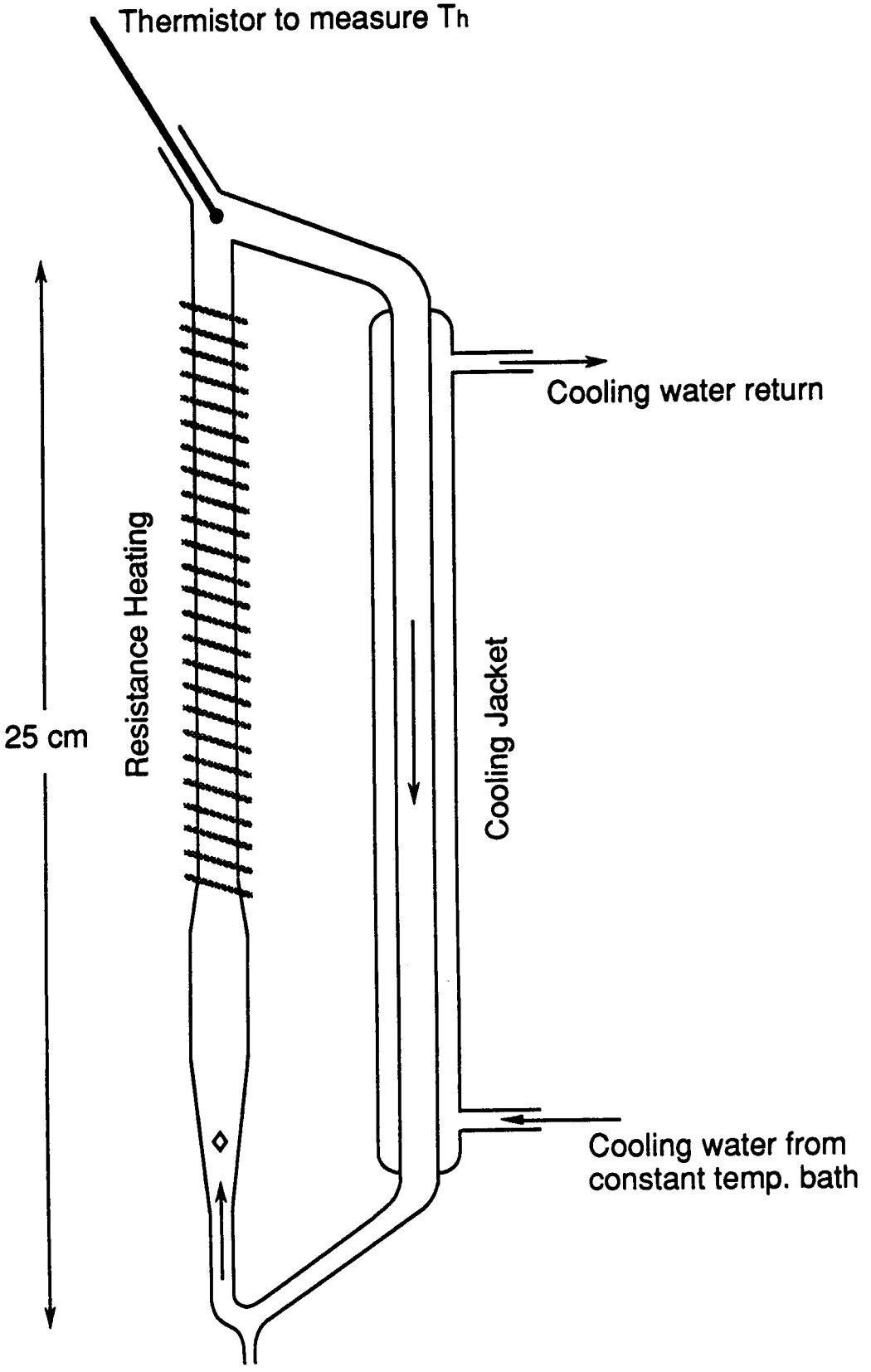

Figure 3. The thermosyphon crystal growth apparatus

are 6mm ID tubing. The port at the top is for filling the apparatus, inserting a thermistor to measure T_h, and for the addition of precipitants, pH buffers, and seed crystals or nuclei. The port at the bottom of the apparatus allows removal of crystals during operation and facilitates draining.

The apparatus is designed for crystallization of materials having normal dependance of solubilities on temperature, with the growth (expansion) chamber at the bottom of the heated section. The lower bend and the section entering the growth chamber are made from 3mm ID tubing. This creates locally a higher velocity to aid the suspension of the crystals and to keep crystals from settling in the lower part of the apparatus. The growth chamber itself varies from 3mm to 10mm ID, with a maximum 7° angle of expansion. This produces a more than 10 fold variation of velocity in the chamber and reduces recirculation. The lower part of the apparatus is insulated so the solution temperature at the site of the suspended crystal is essentially the same as that leaving the bottom of the cooled section, which is the coldest (most supersaturated) fluid in the loop. The velocity is increased or decreased, respectively by increasing or decreasing the temperature difference between the two sides of the apparatus.

To operate this apparatus efficiently, i. e. to set the operating parameters to produce the desired result, one must understand how the temperature distribution in this loop affects the velocity. Additionally, one should be able to make a larger (or smaller apparatus) without relying on trial and error. Due to the more complex geometry of our design and the simplifying assumptions made in existing thermosyphon models, these earlier treatments cannot be used to predict the velocity as a function of temperature in our apparatus. Therefore, a mathematical model was developed to explore different geometries with higher suspension velocities and smaller required solution volumes.

The mathematical derivation, details of which are given in the Appendix, is based on the following considerations. The buoyancy force is integrated around the loop to obtain the flow-driving pressure differential. For steady-state flow this force must equal the overall friction force acting in the opposite direction. The input parameters are the geometry (the length, diameter and positions of the four segments of the apparatus), the physical properties of the solution, and the temperatures at the top of the heating section and at the crystal. The resistance heating section is assumed to have

a constant heat flux boundary condition along its length. The temperature distribution in the cooling section depends on the velocity as well as the thermal diffusivity of the circulating solution. Since it is the temperature distribution that determines the buoyancy force which drives the velocity, the solution is an iterative one. A computer program was written to solve the set of equations and is included in the Appendix.

Velocities in the thermosyphon crystal growth apparatus were measured and compared to those predicted by this model; see Figure 4. Note that the velocities are average velocities based on a 6mm diameter tube. The velocities in the expansion chamber vary from 4 (in the lower 3mm part) to 0.36 (in the upper 10mm part) times these values. We see that the model can be used to predict the velocity with reasonable accuracy. The difference is most likely due to heat transferred to the expansion chamber from the ambient, which is neglected in the model. Since there are no empirical "fitting" parameters in this model, we feel confident that it can be used to predict velocities in other apparatuses of different geometry and size, as well as for solutions with different physical properties.

The downward curvature in Figure 4 is due to changes of the temperature distribution in the cold leg of the loop as the velocity is increased. The thermal entrance length in the cooled section increases with increasing velocity, thus reducing the overall buoyancy force. If the tube were very small in diameter, the thermal diffusivity very high, or the velocity very low, the temperature of the solution entering the cooled tube would quickly (i.e. after a short distance) reach the temperature of the wall. Consequently, many previous thermosyphon models are based on the assumption that the fluid in the entire cold section is at T_w. In the present model, however, full account is made of the developing temperature in the cold section, without assuming that T_w is reached at the sections end.

Figure 5 shows how the temperature distribution in the cooling section relates to the solution velocity . We can see that for a velocity of 0.05 cm/s, the temperature of the fluid is T_w for a majority of the tube's length, while a velocity of 0.2 cm/s spreads the temperature change out over most of the length of the tube. For 0.35 cm/s the thermal entrance length exceeds the length of the tube and the final temperature remains significantly above T_w. This is not only important for the resulting overall bouyancy but also for the supersaturation at the crystal.

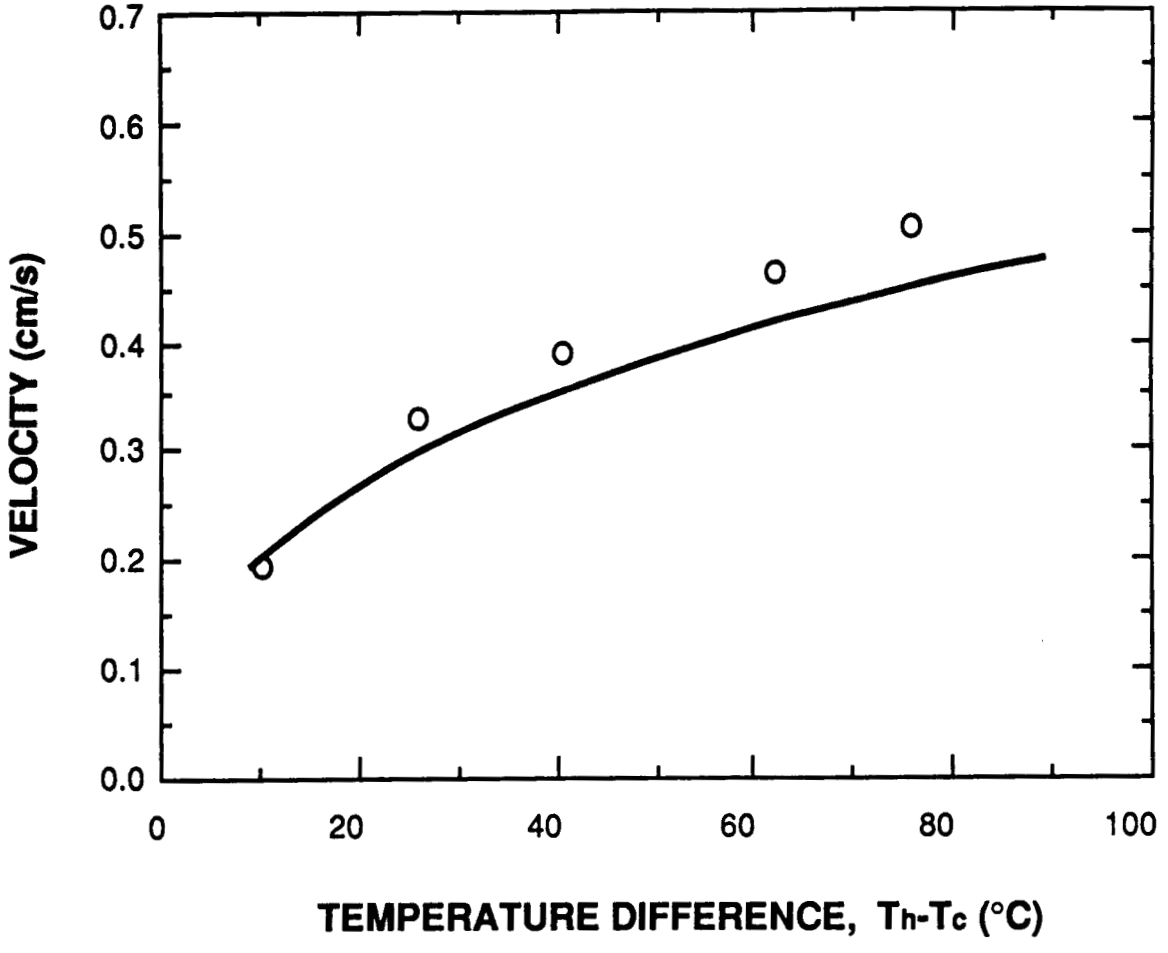

Figure 4. Velocity in the thermosyphon as a function of the temperature difference between the heated section and the cooling jacket temperature. Comparison of experimental values (circles) with model calculations (line).

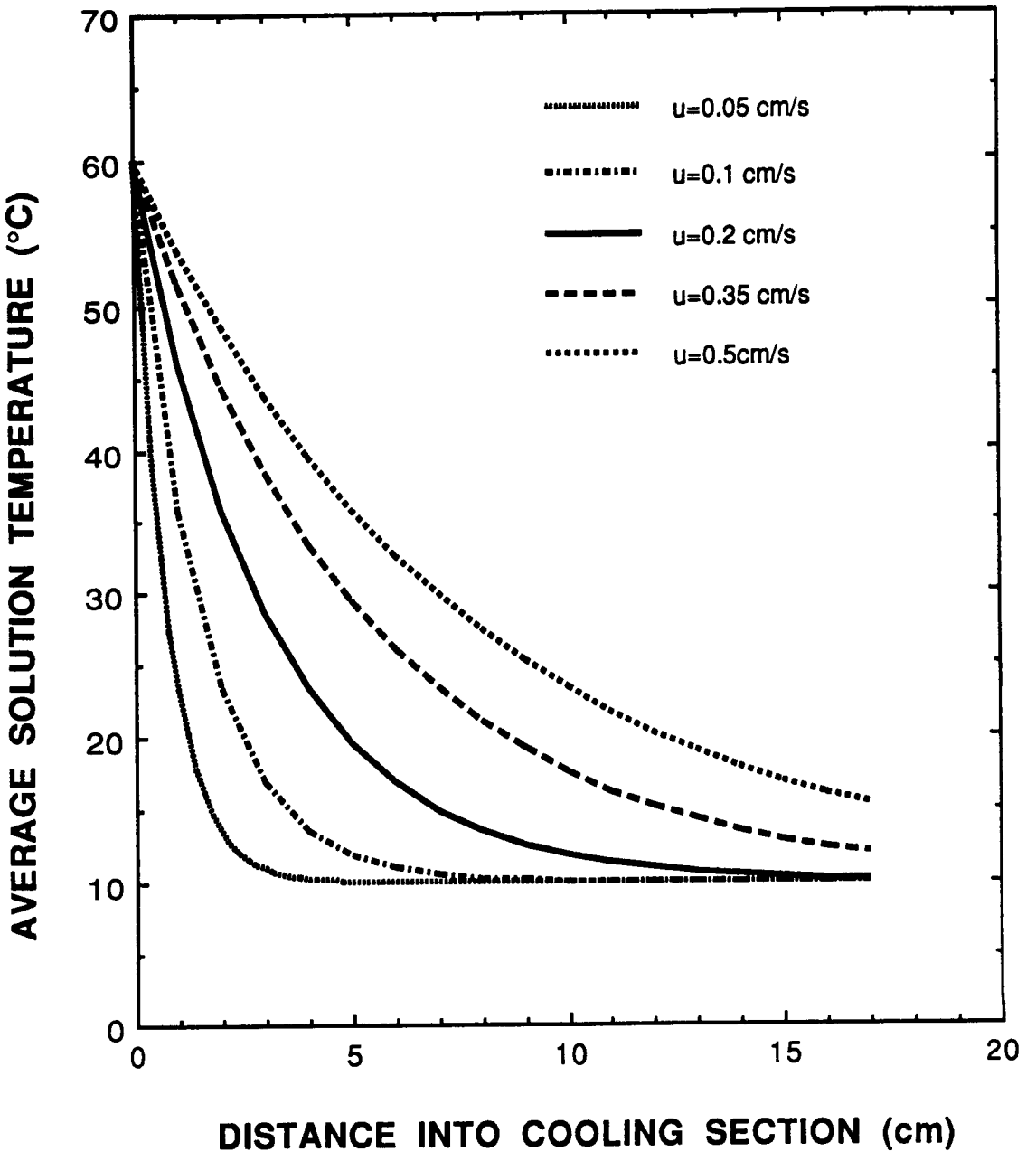

Figure 5. Temperature distribution along the length of the cooled tube for T_h=60°C and T_{wall}=10°C

The effect of the tube diameter on the solution velocity is complicated. Figure 6 shows the velocity as a function of tube diameter for three different values of ΔT. The maximum arises from a combination of two opposing phenomena. For small tubes the viscous forces dominate and the corresponding drag reduces the velocity. For large tubes the thermal entrance length is longer and the effect discussed above becomes significant. Note that the curve for ΔT=30°C (a reasonable value for protein solutions) has its maximum near 6mm, the diameter used in most of the loop in our crystal growth apparatus.

3. Crystallization Results

3.1 Potassium Aluminum Sulfate and Sodium Chloride

Two inorganic systems (NaCl and $AlK(SO_4)_2$) were used to study the characteristics of the apparatus and to develop an "operating procedure" for startup, initiation of growth, and continued growth to the desired size. Several schemes were tried and the most successful one is described here. In this description, T_h and T_c are the temperatures of the hot and cold sides of the apparatus shown in Figure 3. Additionally, T_s is the temperature at which the solution is saturated and ΔT is T_h-T_c.

1) Set ΔT = 3°C with both T_h and T_c, exceeding T_s.
   The flow in the loop recirculates at a low velocity and any nuclei or crystallites are dissolved.
2) Keeping $\Delta T \approx$ 3°C, lower both temperatures until $T_h < T_s$.
   The solution is now supersaturated but not enough to induce spontaneous nucleation.
3) Inject a small amount (<0.05ml) of saturated solution containing seed crystals. 1-10μm crystals were used, but the size is not critical. These crystals are so small that they travel with the fluid around the loop while they are slowly growing.
4) When one or more crystals grow large enough to be trapped in the low velocity section of the growth chamber (typical size is 0.03 mm), increase T_c to the desired growth temperature keeping $\Delta T \approx$ 3°C. Since T_h is now larger than T_s crystals which flow through the growth chamber are dissolved in the heated section.

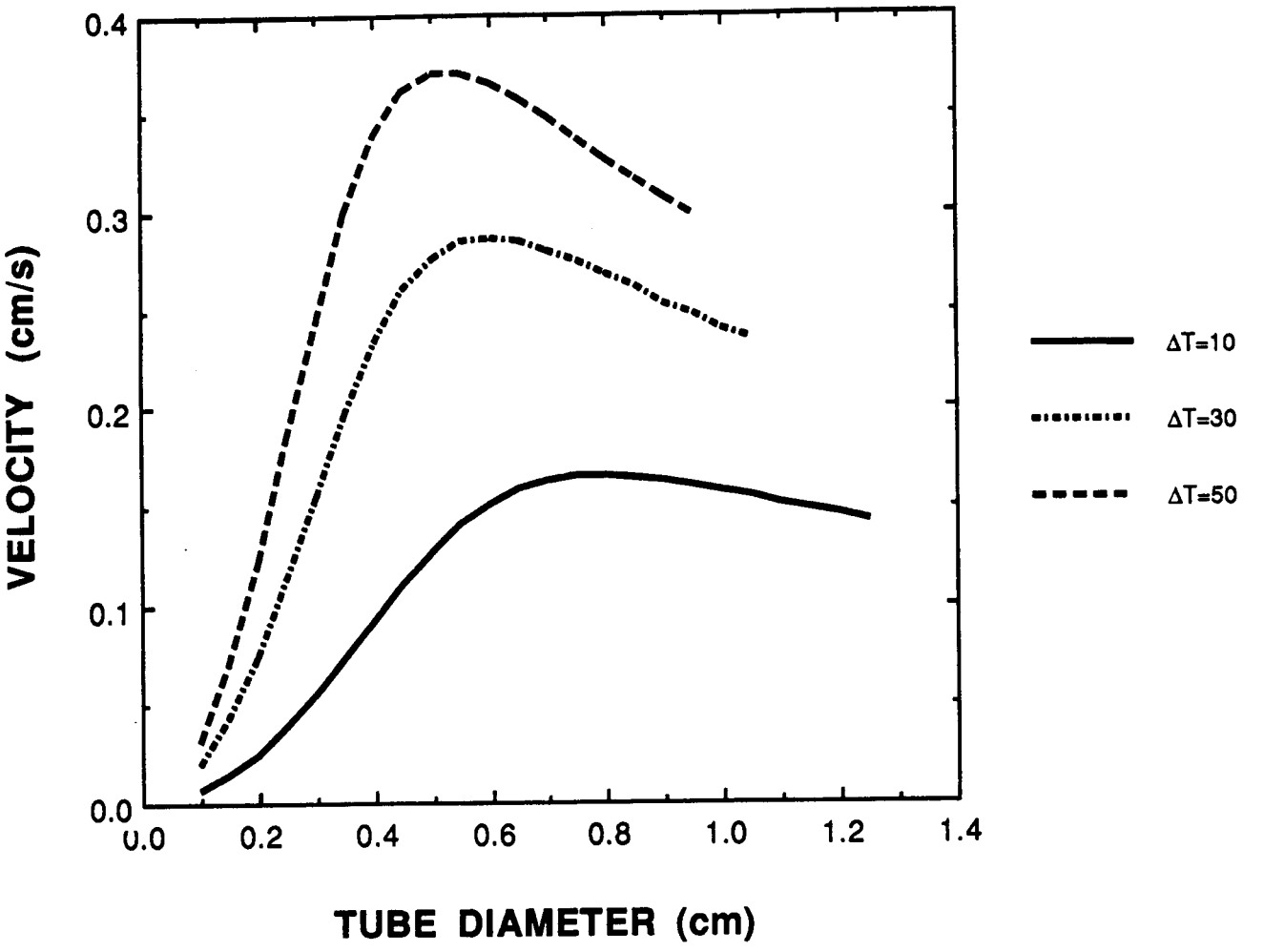

Figure 6. Model calculations for the average solution velocity in the thermosyphon as a funtion of tube diameter.

5) Increasing the ΔT speeds the flow and sweeps the smaller crystals up into the heated section where they are dissolved. Decreasing the ΔT reduces the velocity to let the larger crystals settle down to the lower port where they are removed. This method was used to eliminate all but one crystal.
6) As the crystal in the chamber grows, it will position itself lower in the expansion section where the velocities are higher. As it continues to grow, T_h is increased to increase the velocity. At these higher velocities, the temperature of the solution reaching the crystal is not that of the cooling jacket. Using Figures 4 and 5 for guidance, the cooling jacket temperature is lowered to maintain supersaturation at the crystal.

Crystals of NaCl and $AlK(SO_4)_2$ were grown to 0.2mm and 0.4mm respectively. In light of the high relative density differences of these systems ($\rho_{solid}/\rho_{solution}$ = 1.8 for NaCl and 1.35 for $AlK(SO_4)_2$) compared to that for protein systems ($\approx$1.17 for lysozyme), these results were very promising. During these runs, it was discovered that a very small angle of inclination of the expansion chamber can cause a "bobbing" of the crystal and contact with the wall. It is recommended that the mounting of apparatuses of this type should have provisions for adjusting the inclination. We have also explored in-situ nucleation but the high supersaturation required caused very rapid growth of the crystals immediately after nucleation.

The "wall effect" discussed in Section 2.1 was displayed dramatically in the above runs. When the tiny seeds became visible in the chamber they were in various positions, some low and near the wall, some high and more centered. After elimination of all but one crystal (by the methods discussed above) its position was usually stable and without wall contact, but not necessarily in the center. When a crystal had grown to about 0.25 mm it began to move toward the center, which it reached with about 0.3mm. This was the expected result, as the diameter of the narrowest part of the channel is 3mm.

3.2 Tetragonal Lysozyme

First, a series of experiments were done attempting to grow tetragonal lysozyme crystals from nuclei formed in-situ. The solution compositions

ranged from 40 to 80 mg/ml lysozyme, 2 to 4 weight percent NaCl and were held at pH4.5 with a sodium acetate buffer. The temperatures in the apparatus ranged from 0 to 35°C, with the temperature for nucleation and or growth always below 25°C. These conditions favor the growth of the tetragonal form of lysozyme [11, 12]. The supersaturation required for nucleation and growth was attained either via addition of NaCl (acting as a precipitating agent), or by temperature changes, or by combinations of both.

Nucleation occurred and cystallites were trapped in the expansion chamber. The crystallites had a very narrow size distribution, so the methods discussed above for reducing the number of crystals were not as successful as for the inorganic crystals. In some cases continued nucleation added to this problem. Each of the experiments took at least a week, due to the slow growth rates of lysozyme. The largest crystallites were less than 0.1 mm and did not continue to grow even under supersaturation conditions producing continued nucleation. Microscopic examination showed that the crystallites lacked well defined facets.

Previous to this research, it was not known whether the continuous circulation of the solution during the time of a typical experiment would denature the protein in solution. We found that it took 2-3 weeks for any noticeable denaturization of the protein to occur. After 3 weeks, the amount of insoluble denatured protein formed was small and appeared as a thin "haze" on the inner glass surfaces and caused some cloudiness of the solution. It was suspected that this was not the cause for the growth cessation of the crystallites. This was confirmed when solutions which had been circulating for more than three weeks grew large crystals (on the walls) when the circulation was stopped and the apparatus held at a constant temperature.

Next a series of experiments were done attempting continued growth of introduced tetragonal lysozyme crystal seeds. The seeds were produced in standing or hanging drops and were transferred to the thermosyphon via an Eppendorf pipet. The solutions used in these experiments had compositions which will produce growth of lysozyme crystals in batch systems but would not readily cause spontaneous nucleation.

A set of stagnant control experiments were performed at various constant temperatures simultaneously to these thermosyphon runs. These batch experiments were done with the same solution in them as the

thermosyphon and were seeded at the same time with seeds from the same sandwich (or hanging) drop. These "control" experiments produced important results of their own and were essential for developing succesful seed transfer techniques. It was found that if the seed crystal undergoes a sudden temperature change of more than a few degrees during the transfer, it will not grow thereafter. Additionally when the solution to which the seed was transferred had a different salt concentration, no growth occured. We developed the following transfer technique:

1) Nucleate and grow seed crystals in a hanging drop.
2) Move the cover slip with the hanging drop to a new reservoir which has the (lower) NaCl concentration of the solution in the thermosyphon.
3) Allow 2 days for equilibration before the crystal is transferred with a pipet.

Seed crystals transferred to temperature controlled batch cells with this technique showed uninhibited growth.

During transfer to the thermosyphon, the apparatus was held at a uniform, ambient temperature with no circulation. The temperature in the thermosyphon was then slowly changed to the desired operating conditions (over a period of hours) to start the flow and suspend the crystal. There was no measurable growth of the suspended seeds during the time that the stagnant controls showed significant growth. Experiments varied from 5 to 20 days. When supersaturation was increased by lowering the temperature or addition of NaCl, there still was no growth and the facets of the seeds became "frosted". Two possible reasons for this behavior are:

1) Kinetic, due to the repeated heating and cooling the solution undergoes as it circulates. It has been speculated (but not published) that lysozyme growth units are larger than monomers and that there is a "preclustering" necessary before attachment. If the kinetics of this preclustering are slow, it may be hampered by the oscillating temperatures.

2) Mechanical, due to the crystal being suspended by the drag forces of the fluid around it. It is possible that the shear forces on the surface of the crystal will not allow the growth units to attach (the strength of bonding in protein crystals is relatively unknown).

Reason 2) would have very important implications for the growth of protein crystals in space as well as on earth. One of the main reasons cited for growing crystals in space is the reduction of bouyancy induced convection. These thermosyphon growth experiments appear to indicate that convection has an adverse affect and can cause "growth cessation."

3.3 Orthorhombic Lysozyme

Similar tests were conducted under conditions favorable for the growth of the orthorhombic form of lysozyme. In contrast to results obtained with the tetragonal form, there was no cessation of growth. After in-situ nucleation, and without any change of conditions (temperature or concentration) a single crystal became visible in the expansion chamber. As it grew, T_h was raised to increase the velocity and to keep the crystallite suspended. It grew to a size of 1.5x0.5x0.2 mm before it was removed. At this time a few other smaller crystals had appeared and were growing. These were also removed successfully and 2 days later there were more, in the size range 0.1-0.5mm and still growing.

We feel that under these conditions (or improved ones) many crystals of ideal size for x-ray diffraction can be grown sequentially from the same solution. Once the solution becomes depleted, the temperature can be lowered or the NaCl concentration increased to "squeeze out" more crystals. We speculate that the reason that the growth of orthorhombic crystals is not inhibited (like that of the tetragonal form) is that the bond strength is greater.

4. Summary and Conclusions

This research proceeded along the lines of the task schedule in the original proposal. A flow expansion chamber was designed to suspend growing crystals and was tested under forced flow conditions by first suspending plexiglass particles and then NaCl and $AlK(SO_4)_2$ crystals in their saturated solutions (tasks 1,2). These tests determined the range of velocities required to suspend crystals up to the size necessary for x-ray diffraction (0.3mm-1mm). Estimates based on earlier models and lab experiments showed that the required velocity could be attained by buoyancy induced convection in a thermosyphon loop (tasks 3,4). Since there were large discrepancies between the velocities predicted by earlier

models [7] and experiments in a simple thermosyphon geometry, a mathematical model was developed which allowed a more realistic description of the temperature distribution in the loop and thus of the buoyancy force which drives the flow. This model was used to design a thermosyphon crystal growth apparatus.

A thermosyphon crystal growth apparatus was constructed which was used to grow crystals of NaCl and $AlK(SO_4)_2$ (task 5). The high diffusivities of these materials led to "ripening" processes which allowed single crystals to be isolated in the expansion chamber easily. The suspension limit for these materials was only 0.2 mm and 0.4 mm respectively due to the large density difference between the crystals and their saturated solutions. Note that this apparatus was designed to grow protein crystals of 1mm or less and the solution volume was limited. To grow other more dense materials (inorganics, organic non-linear optical materials etc.) the apparatus could be scaled up for higher velocities and to accomodate larger crystals. Included in this report are details of the apparatus designed during this research as well as guidelines for the design of such systems for other materials with different crystal and solution properties.

Lysozyme solutions were used in the next series of experiments (task 6). Conditions favorable for in-situ nucleation of the tetragonal form of lysozyme were tried first. The crystallites had a narrow size range which made it difficult to reduce the number in the growth chamber, and they did not grow larger than 0.1 mm. When (larger) tetragonal seeds were transferred to the apparatus, they showed no measurable growth, even though seeds transferred to stagnant control cells showed uninhibited growth.

When conditions favorable for the growth of orthorhombic lysozyme were used, there was no cessation of growth and the crystals grew to the maximum suspension limit (1.5 mm). Several crystals were grown sequentially and removed without visible damage. During the removal of a crystal, less than 0.1 ml is lost, with the remaining solution used to grow more crystals.

The technology developed during this research is a viable crystal growth method. It can be used to produce crystals of orthorhombic lysozyme large enough for x-ray diffraction. Which other proteins it could be used for is not clear and depends, at least partially, on the reasons for the hindered growth

of the tetragonal form (see Section 3.2). Additionally a scaled up version can be used for the growth of larger crystals of many other solution grown materials.

There was mutually beneficial communication with protein researchers at UAH and Marshall Space Flight Center and a scientific publication is in preparation (task 7).

5. APPENDIX: Mathematical Model for the Solution Velocity in the Thermosyphon.

Nomenclature	
D	diameter of the tube
L	total length of the loop
S	length variable measured from the bottom of the heated section
S_1	length to the top of the heated section
S_2	length to top of cooled section
S_3	length to the bottom of the cooled section
T	mean fluid temperature (averaged across the cross section)
T_0	fluid temperature leaving the bottom of the cold section
T_h	fluid temperature at the top of the heated section
T_w	wall temperature in the cooling section
U	average cross-sectional velocity
x	dimensionless distance
α	thermal diffusivity of the fluid
μ	dynamic viscosity of the fluid
τ_w	shear stress on the wall
θ	angle between the flow direction and the gravity vector

The equations for conservation of mass and momentum are

$$\frac{\partial \rho}{\partial t} + \frac{\partial (\rho U^2)}{\partial S} = 0 , \tag{1}$$

$$\frac{\partial \rho U}{\partial t} + \frac{\partial (\rho U^2)}{\partial S} = - \frac{\partial p}{\partial S} - \rho\, g \cos\theta - \frac{2}{r} \tau_w . \tag{2}$$

If we assume steady state conditions, (1) indicates that the mass flux ρU is constant along the loop. Integrating (2) around the length of the loop gives

$$g \int_0^L \rho \cos\theta \, dS + \frac{2}{r} \int_0^L \tau_w \, ds = 0. \tag{3}$$

For Poiseuille flow in tubes, the shear stress at the wall is

$$\tau_w = \frac{8\mu U}{D}. \tag{4}$$

If we let $\rho=\rho_0(1-\beta(T-T_0))$ and subsitute (4) into (3) we get

$$-\rho_0 \beta g \int_0^L T \cos\theta \, dS = \frac{32\mu UL}{D^2}. \tag{5}$$

Due to the changing boundary conditions along the loop, the left side integral is done piecewise; the pieces corresponding to the four sections of the apparatus.

$$\int_0^L T \cos\theta \, dS = \int_0^{S_1} T \cos\theta \, dS + \int_{S_1}^{S_2} T \cos\theta \, dS +$$

$$\int_{S_2}^{S_3} T \cos\theta \, dS + \int_{S_3}^{L} T \cos\theta \, dS . \tag{6}$$

For the section heated by electrical resistance, $\theta=\pi$ and and we assume a constant heat flux. This means that for $0 \le S \le S_1$, average temperature varies linearly with distance through the tube.

$$T = T_0 + (T_h - T_0)\left(\frac{S}{S_1}\right). \tag{7}$$

So,

$$\int_0^{S_1} T \cos\theta \, dS = - S_1 (T_0 - (T_h - T_0)/2). \tag{8}$$

For the upper part of the loop the temperature is T_h and

$$\int_{S_1}^{S_2} T \cos\theta \, dS = - \int_{H_{S_1}}^{H_{S_2}} T_h dH = - T_h (H_{S_2} - H_{S_1}) , \qquad (9)$$

where H_{S2}-H_{S1} is the height differential between the top of the cooled section and the top of the heated section.

For the cooled section of the loop, $\theta=2\pi$ and the temperature is a function of distance through the section, temperature of the cooling wall, T_c, and the thermal diffusivity of the solution, α. The solution of the energy equation for the thermal entry region of a tube with constant surface temperature is given in [13]. This series solution can be approximated by

$$\frac{T - T_w}{T_h - T_w} = 0.913(10)^{-3.5(x)} . \qquad (10)$$

Here, x is the dimensionless distance defined as $x=(2\alpha s)/(UD^2)$. Note that, although there is almost a 9% error at x=0, the error becomes much smaller when x>0.05. Solving (10) for the temperature gives

$$T = 0.913(T_h - T_w)10^{\left(\frac{-7\alpha}{UD^2} S\right)} + T_w , \qquad (11)$$

where $a= (-7\alpha)/(UD^2)$ and thus

$$\int_{S_2}^{S_3} T \cos\theta \, dS = \frac{0.913(T_h - T_w)}{a(\log 10)} (10^{a(S_3 - S_2)} - 1) + T_w(S_3 - S_2) . \qquad (12)$$

For the lower section of the loop, the temperature is assumed constant at the growth temperature T_0, so we write

$$\int_{S_3}^{L} T \cos\theta \, dS = - \int_{S_3}^{H_L = 0} T_0 \, dH = T_0 \, H_{S_3} . \qquad (13)$$

Subsituting (8),(9),(12), and (13) into (6) gives

$$\int_0^L T\cos\theta\, dS = -S_1\left(T_0 + \frac{T_h - T_0}{2}\right) - (H_{S_2} - H_{S_1})(T_h) +$$

$$+ \frac{0.913(T_h - T_w)}{a(\log 10)}\left(10^{a(S_3 - S_2)} - 1\right) + T_w(S_3 - S_2) + H_{S_3} T_0 . \qquad (14)$$

We call this term the "geometrical factor", ϕ, and write (5) as

$$\frac{32\mu UL}{D^2} + \rho_0\beta g\phi = 0. \qquad (15)$$

Equation (11) tells us that at the bottom of the cooled section

$$T_0 = 0.913\,(T_h - T_w)\,10^{a(S_3 - S_2)} + T_w . \qquad (16)$$

Rearranging,

$$T_w = \frac{T_0 - 0.913\,T_h\,10^{a(S_3 - S_2)}}{1 - 0.913\cdot 10^{a(S_3 - S_2)}} . \qquad (17)$$

A small computer program, used to solve (15) by the method of regula falsi and is presented below. Upper and lower bounds on the velocity, U1 and U2 respectively, are used to start. For each iteration, the velocity is used to determine the the temperature distribution (and thus the bouyancy forces), (15) is checked, and a new more accurate velocity is calculated. This process continues until a tolerance is met.

```
REM D is the inside diameter of the tube
REM L is the total length of the apparatus
REM beta is the coefficient of expansion ( /C)
REM mu is the dynamic viscosity of the solution (gm/cm/sec)
REM k is the thermal conductivity  (cal/sec/cm/C)
REM Cp is the heat capacity 1cal/gm/C
REM U is the average velocity of the solution
REM ro is the density of the solution
REM s is the distance variable in the flow direction
REM s=0 at the bottom of the heated section
REM s=s1 at the top of the heated section
REM s=s2 at the top of the cooled section
REM s=s3 at the bottom of the cooled section
REM H is the height variable (0 at s=0)
REM Hs2 is the height of the top of the cooled section
REM Tw is the temperature of the cooling jacket
REM Th is the temperature at the top of the heated zone
REM T0 is the temperature at the bottom of the heated zone
REM DT is the change in temperature in the column
REM no correction has been made for the drag on the particle
reducing the velocity


OPEN "CLIP:" FOR OUTPUT AS #1
READ mu,ro,beta,g:                    REM input solution properties
DATA  0.0098,1.074,0.000225,981
READ T0:                                        REM input growth
temperature
DATA 20.0
READ Cp,k,s1,s2,s3,L
DATA  1,0.00148,22.5,36.5,53.5,73
READ DT1,DT2,DTstep,D1,D2,Dstep:      REM input ΔT and Diameter
ranges
DATA  4,80,2,0.4,0.8,0.2

FOR D = D1 TO D2 STEP Dstep
PRINT  " "
PRINT  " "
PRINT  "For an inner tube diameter of",D;"cm"
PRINT  " "
PRINT  "          velocity (cm/s)";"   Th-To (°C)","required Tw (°C)"
FOR DT = DT1 TO DT2 STEP DTstep
```

```
U1=.002:                          REM minimum guess for velocity
U2=1.5:                           REM maximum guess for velocity
FB=1:                              REM initialize convergence tolerance

DEF  FNT=(.397*(DT+T0-Tw)/a)*(10^(a*(s3-s2))-1)+Tw*(s3-s2)
WHILE (ABS(FB)>.001):      REM check convergence
     a=-7*k/(ro*U1*(D^2)*Cp)
      Tw=T0-DT*(10^(a*(s3-s2))/(1-(10^(a*(s3-s2)))))
     phi= -s1*(T0+DT/2)-(-3.81)*(T0+DT)+FNT+(-1.27)*T0
      FU1=-D^2*ro*beta*g*phi/(32*mu*L)-u1

     a=-7*k/(ro*U2*(D^2)*Cp)
      Tw=T0-DT*(10^(a*(s3-s2))/(1-(10^(a*(s3-s2)))))
     phi= -s1*(T0+DT/2)-(-5)*(T0+DT)+FNT+(-.5)*T0
      FU2=-D^2*ro*beta*g*phi/(32*mu*L)-u2

    LET B=U1-FU1/((FU2-FU1)/(u2-u1))
     a=-7*k/(ro*b*(D^2)*Cp)
      Tw=T0-DT*(10^(a*(s3-s2))/(1-(10^(a*(s3-s2)))))
     phi= -s1*(T0+DT/2)-(-5)*(T0+DT)+FNT+(-.5)*T0
      FB=-D^2*ro*beta*g*phi/(32*mu*L)-B

  IF (ABS(FU1-FB)<ABS(FU1)) THEN U1=B ELSE U2=B
WEND
PRINT  USING"########.### ";B,DT,Tw:          REM print  to screen
REM print #1,  USING"###.### ";D,B,DT,Tw:        REM  print  raw
data  to  clipboard

NEXT DT
NEXT D
END
```

For an inner tube diameter of 0.4 cm

velocity (cm/s)	Th-To (°C)	required Tw (°C)
0.072	4.000	20.000
0.090	6.000	20.000
0.107	8.000	20.000
0.124	10.000	20.000
0.140	12.000	20.000
0.155	14.000	20.000
0.170	16.000	20.000
0.184	18.000	20.000
0.198	20.000	20.000
0.211	22.000	20.000
0.224	24.000	19.999
0.236	26.000	19.999
0.248	28.000	19.998
0.259	30.000	19.997
0.271	32.000	19.995
0.282	34.000	19.992
0.292	36.000	19.989
0.302	38.000	19.985
0.312	40.000	19.979
0.322	42.000	19.972
0.331	44.000	19.965
0.340	46.000	19.955
0.349	48.000	19.944
0.358	50.000	19.931
0.367	52.000	19.917
0.375	54.000	19.900
0.383	56.000	19.882
0.391	58.000	19.861
0.399	60.000	19.838
0.406	62.000	19.813
0.414	64.000	19.786
0.421	66.000	19.756
0.428	68.000	19.724
0.435	70.000	19.691
0.442	72.000	19.654
0.448	74.000	19.614
0.455	76.000	19.572
0.462	78.000	19.527
0.468	80.000	19.480

For an inner tube diameter of 0.6 cm

velocity (cm/s)	Th-To (°C)	required Tw (°C)
0.138	4.000	19.998
0.162	6.000	19.991
0.183	8.000	19.974
0.201	10.000	19.946
0.217	12.000	19.903
0.232	14.000	19.846
0.245	16.000	19.774
0.258	18.000	19.686
0.270	20.000	19.582
0.281	22.000	19.462
0.291	24.000	19.327
0.301	26.000	19.179
0.310	28.000	19.014
0.319	30.000	18.834
0.328	32.000	18.640
0.336	34.000	18.431
0.344	36.000	18.214
0.351	38.000	17.979
0.359	40.000	17.730
0.366	42.000	17.468
0.372	44.000	17.199
0.379	46.000	16.912
0.386	48.000	16.613
0.392	50.000	16.301
0.398	52.000	15.978
0.404	54.000	15.649
0.410	56.000	15.303
0.416	58.000	14.946
0.421	60.000	14.576
0.427	62.000	14.196
0.432	64.000	13.814
0.437	66.000	13.412
0.442	68.000	13.000
0.447	70.000	12.578
0.452	72.000	12.154
0.457	74.000	11.711
0.462	76.000	11.258
0.466	78.000	10.795
0.471	80.000	10.322

For an inner tube diameter of 0.8 cm

velocity (cm/s)	Th-To (°C)	required Tw (°C)
0.188	4.000	19.818
0.207	6.000	19.633
0.222	8.000	19.394
0.236	10.000	19.103
0.249	12.000	18.768
0.260	14.000	18.390
0.270	16.000	17.967
0.280	18.000	17.511
0.289	20.000	17.018
0.298	22.000	16.484
0.306	24.000	15.922
0.314	26.000	15.327
0.321	28.000	14.693
0.328	30.000	14.035
0.335	32.000	13.346
0.342	34.000	12.626
0.349	36.000	11.869
0.355	38.000	11.090
0.361	40.000	10.282
0.368	42.000	9.444
0.374	44.000	8.577
0.380	46.000	7.671
0.385	48.000	6.746
0.391	50.000	5.791
0.397	52.000	4.806
0.402	54.000	3.791
0.408	56.000	2.746
0.414	58.000	1.670
0.419	60.000	0.563
0.425	62.000	-0.577
0.430	64.000	-1.748
0.436	66.000	-2.953
0.441	68.000	-4.192
0.446	70.000	-5.454
0.452	72.000	-6.763
0.457	74.000	-8.110
0.463	76.000	-9.483
0.468	78.000	-10.909
0.474	80.000	-12.363

6. References

[1] G. G. **Stokes**, On the Effect of the Internal Friction of Fluids on the Motion Pendulum *Trans. Cam. Phil. Soc.* **9** (1851) 8.

[2] L. Schiller and A. Nauman, Über die grundlegenden Berechnungen bei der Schwerkraftaufbereitung. *Z. Ver. deut. Ing.* **77** (1933) 318.

[3] H. A. Becker, The Effects of Shape and Reynolds Number on Drag in the Motion of a Freely Oriented Body in an Infinite Fuid. *Can. J. Chem. Eng.*, **37** (1959) 85.

[4] R. Ladenburg, Über den Einfluss von Wänden auf die Bewegung einer Kügel in einer reibenden Flüssigkeit. *Ann. Phys.* **23** (1907) 447.

[5] Y. Zvirin, A Review of Natural Convection Loops in Pressurized Water Reactors and Other Systems. *Nucl. Eng. Design* **67** (1981) 203.

[6] A. Mertol and R. Greif, A Review of Natural Circulation Loops. S. Kakac, W. Aung, and R. Viskanta (ed.) *Natural Convection: Fundamentals and Applications*. (Hemisphere, New York 1985) 1033.

[7] H. F. Creveling, J. F. DePaz, J. Y. Baladi, and R. J. Schoenhals, Stability Characteristics of a Single-phase Free Convection Loop. *J. Fluid Mech.* **67** (1975) 65.

[8] P. S. Damerell and R. J. Schoenhals, Flow in a Toroidal Thermosyphon with Angular Displacement of Heated and Cooled Sections. *J. Heat Transfer* **101** (1979) 672.

[9] R. Grief, Y. Zvirin, and A. Mertol, The Transient and Stability Behavior of a Natural Convection Loop. *J. Heat Transfer* **101** (1979) 684.

[10] J. E. Hart, Observations of Complex Oscillations in a Closed Loop Thermosyphon. *J. Heat Transfer* **107** (1985) 839.

[11] P. Jollés and J. Berthou, High Temperature Crystallization of Lysozyme: an Example of Phase Transition. *FEBS Letters*, **23** (1972) 21.

[12] S. B. Howard, P. J. Twigg, J. K. Baird, and E. J. Meehan, *J. Crystal Growth* **90** (1988) 94.

[13] W. M. **Kays** and M. E. Crawford, *Convective Heat and Mass Transfer*, McGraw Hill, New York, 1980.